# Supporting information

# A hydrophilic porphyrin-based COF to reduce CO2 and nitrite in situ for photoelectrochemical catalysis synthesis of urea

## Materials

All chemicals and reagents were used without any further purification. 4-formylphenylboronic acid, 10,15,20-tetrakis(4-bromophenyl)-porphyrin (TBPP), tetrakis(tri-phenylphosphine) palladium catalyst (10 %$Pd(PPh_3)_4$), Sodium hydroxide, Dopamine(DA), Resveratrol(Res), Dichlorome-thane(DCM) and potassium carbonate ($K_2CO_3$) were purchased from Anergy Chemistry, N,N-Dimethylformamide(DMF), Toluene, Hydrogen peroxide(30% $H_2O_2$), Indophenol blue reagent and Nassler`s reagent were purchased from Shanghai Amperexperiment Technology. Deionized water was used in all experiments.

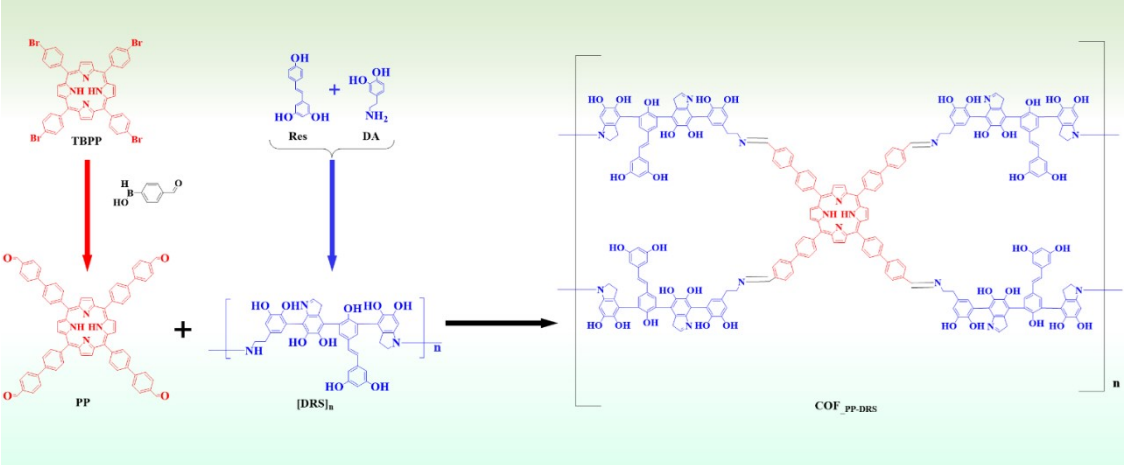


Fig.S1 Synthesis of $COF_{PP\text{-}DRS}$

## Experimental section

### Synthesis

**Synthesis of 5, 10, 15, 20-tetrakis(4-formyl-biphenyl)-porphyrin (PP)**

TBPP (1.20 g, 1.29 mmol) and 4-formylphenylboronic acid (1.40 g, 9.34 mmol) were dissolved in 80 mL DMF, 160 mL toluene and 40 mL $H_2O$ in a three-necked flask, then added 10 % $Pd(PPh_3)_4$ (0.18 g，0.15 mmol). The solution was heated to reflux and reacted for 72 hours under $N_2$. The product was collected as violet black cake by decompression filtration. The crude product was washed with DCM. The mass of synthesized pure PP products is 1.21 g. Its IR profile was shown in Figure S8.

**Synthesis of $COF_{PP\text{-}DRS}$**

The synthesis pathway of $COF_{PP\text{-}DRS}$ is shown in Fig. S1. DA (0.01 g, 0.06 mmol) and Res (0.035 g, 0.15 mmol) were dissolved in 40 mL MeOH, then 1.0 mL 4% NaOH solution was added with 0.08 mL of 30% $H_2O_2$ solution, and the reaction was continued for 2 h. The color of the solution gradually deepened to yellowish brown due to the polymerization of DA and Res. 10 mg of PP was added to the solution, and after reaction for 1 h, 2.0 mL 4% NaOH solution with 0.02 mL 30% $H_2O_2$ solution was added at final. After reaction for 5 h, the solution was dialyzed in pure water for 16 h to obtain $COF_{PP\text{-}DRS}$ solution, which

was concentrated and freeze-dried under low pressure to obtain $COF_{PP\text{-}DRS}$ and yield was 0.04 g. Its IR profile was shown in Figure S8.

### Physical characterization of $COF_{PP\text{-}DRS}$

$COF_{PP\text{-}DRS}$ solution which concentrations of 1.00 mg/mL was subjected to UV optical characterization in a U-3900 model UV spectrophotometer, and $COF_{PP\text{-}DRS}$ solution which concentrations of 0.06 mg/mL was subjected to fluorescence optical characterization in an Agilent Cary Eclipse fluorescence spectrometer.

### Photoreactivity experiments and $CO_2RR$ and $NO_2^-RR$ capabilities

The photoelectric activity of $COF_{PP\text{-}DRS}$ was evaluated in an H-type electrolytic cell with $CO_2RR$ and $NO_2^-RR$ capabilities. $KHCO_3$ or $KNO_2$ solution at different concentrations was the electrolyte solution, and the system was bubbled with Ar for 25 min to remove dissolved oxygen. The photoelectric activity of $CO_2RR$ and $NO_2^-RR$ capability were tested under the condition of applying a voltage of -0.75 V versus Saturated calomel electrode (vs. SCE) with the $COF_{PP\text{-}DRS}$ -ITO as the working electrode, saturated calomel electrode as the reference electrode, and platinum sheet electrode as the counter electrode.

### Photoelectrocatalytic $CO_2$ reduction with charge impedance capability

The photoelectrocatalytic performance and charge impedance ability of $COF_{PP\text{-}DRS}$ were evaluated in an H-type electrolytic cell. 0.5 M $KHCO_3$, 0.2 M $KNO_2$ mixed solution or 0.1 M $NaSO_4$ solution was the electrolyte solution, and the system was bubbled with Ar for 25 min to remove dissolved oxygen. $COF_{PP\text{-}DRS}$ -ITO was used as the working electrode, saturated mercuric glycidic electrode as the reference electrode, and platinum-chip electrode as the counter electrode to apply a voltage of - 0.75 V (vs. SCE) during the photoelectrocatalytic $CO_2$ reduction under the condition of continuous $CO_2$ drumming. The liquid products generated during the reduction process were detected by nuclear magnetic resonance (NMR), indophenol blue and Nessler`s reagent method, then the gaseous products were detected by gas chromatography. The charge impedance capability of the materials was tested at open circuit voltage values.

### Physical properties of $COF_{PP\text{-}DRS}$

The UV and fluorescence spectra were analyzed to investigate the optical properties of the material. The UV spectra (Fig. S2) showed that PP had a Soret band at 413 nm and four Q bands at 512, 548, 589, and 644 nm, which belong to the characteristic absorption of porphyrin, and the copolymer( $[DRS]_n$) had continuous UV absorption bands at 229, 285, 308, 289, and 446 nm, which suggested that the polymer could efficiently absorb utilizing photoelectrons from 200 to 450 nm, which was conducive to photoelectrocatalytic reduction. The strong UV absorption at 285, 322, and 432 nm, and the strong jump at 432 nm suggested the existence of a classical porphyrin structure. A large number of π-π conjugated structure of the benzene ring in $COF_{PP\text{-}DRS}$, which leaded to an increase in the density of electron cloud of the compound and energy required for electron jump was greatly improved. The energy required for the electron cloud of $COF_{PP\text{-}DRS}$ was reduced. Then the stability of $COF_{PP\text{-}DRS}$ was greatly improved, leading to the disappearance of the Q-band absorption and the redshift of the Soret band form 413 nm to 432 nm, which indicated that $COF_{PP\text{-}DRS}$ broadens the UV absorption range and obviously improves the absorption of light. That was conducive to its photoelectrocatalytic reduction of $CO_2$.

The fluorescence spectra (Fig. S3) showed that the maximum excitation wavelength of $COF_{PP\text{-}DRS}$ was 440 nm, and the emission wavelength of the fluorescence peaks was at 488 nm, belong to the characteristic fluorescence emission peaks of porphyrin rings S1 to S0, which corresponded to its UV maximum absorption peaks. The fluorescence profiles of $COF_{PP\text{-}DRS}$ showed strong fluorescence intensity under laser excitation from 410 to 460 nm, which indicated that $COF_{PP\text{-}DRS}$ had a wide light absorption range and the strongest photoelectron utilization ability for laser light at a wavelength of 440 nm.

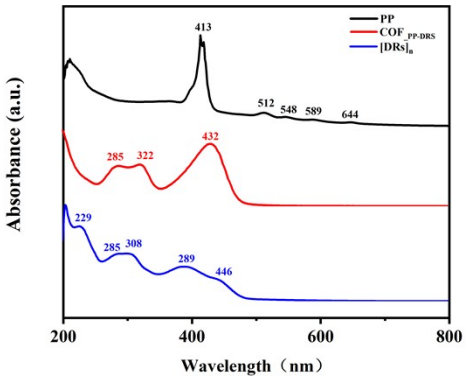


Fig.S2 UV-visible diffuse reflectance spectra of $COF_{PP\text{-}DRS}$

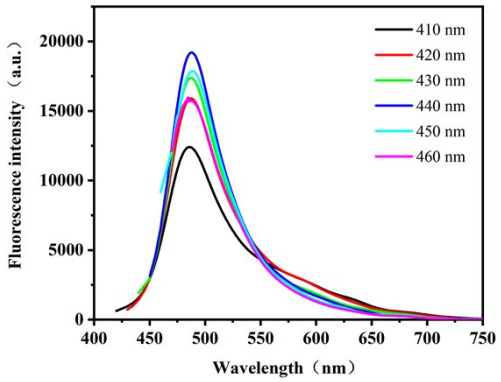


Fig.S3 Fluorescence spectra of $COF_{PP\text{-}DRS}$

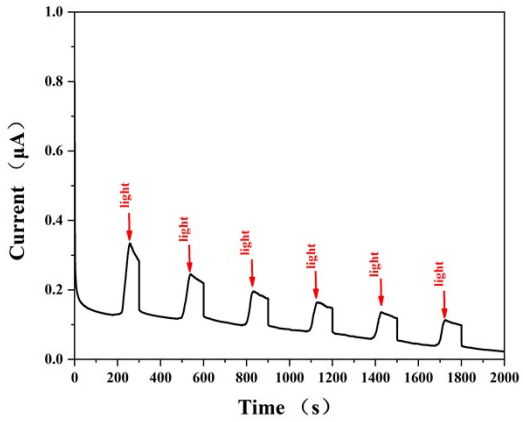


Fig.S4 I-T curve of $COF_{\_PP\text{-}DRS}$ under different illumination conditions

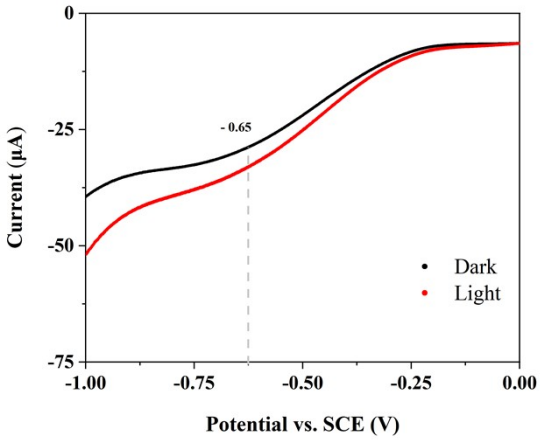


Fig.S5 CV curve of $COF_{\_PP\text{-}DRS}$ under different illumination conditions

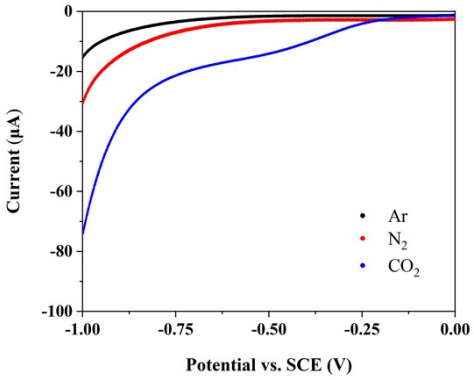


Fig.S6 CV curves of $COF_{\_PP\text{-}DRS}$ under different gas atmospheres

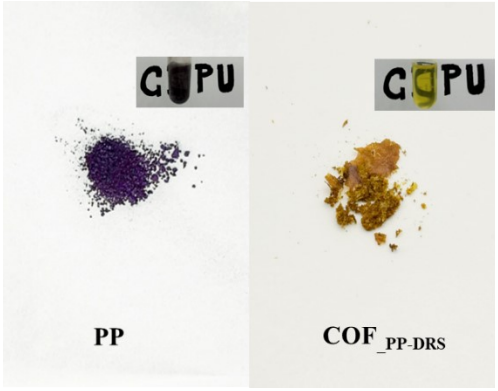


Fig.S7 Morphology of PP (left) and $COF_{\_PP\text{-}DRS}$ (right) and the illustration is a diagram of its state in water

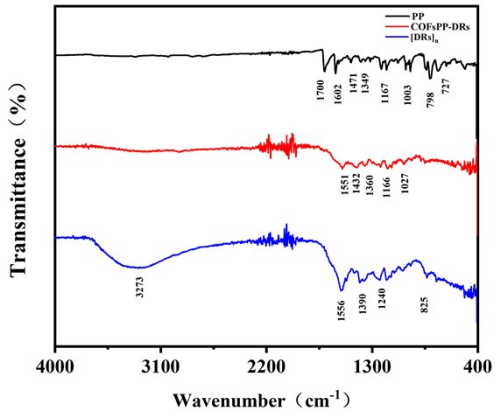


Fig.S8. Infrared Spectroscopy of COFsPP-DRS

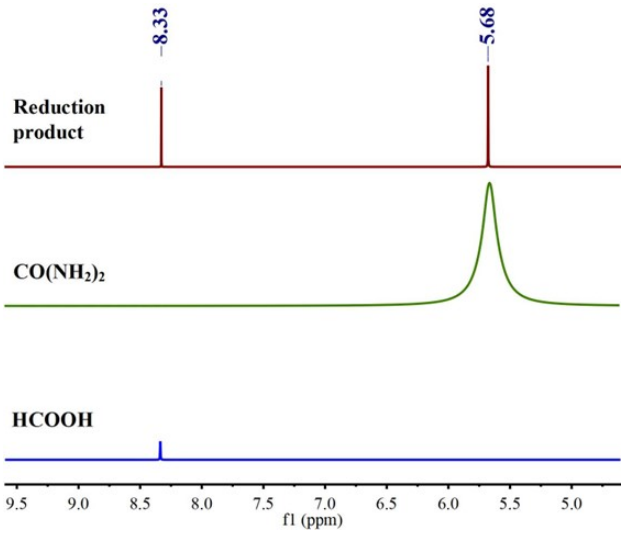


Fig.S9. The NMR spectrum of reduction products

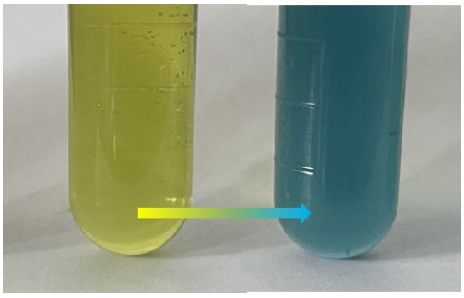

Fig.S10. Diagram of indigophenol blue colorimetry

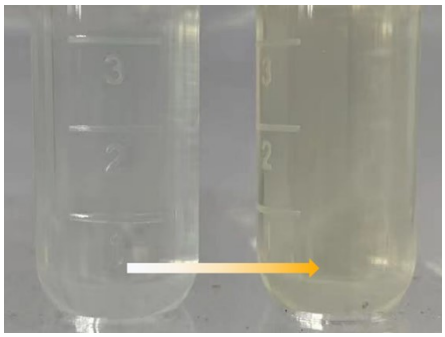

Fig.S11. Diagram of sample tested by Nesser's reagent